DIOMIGNITE: NATURAL $Li_2B_4O_7$ FROM THE TANCO PEGMATITE, BERNIC LAKE, MANITOBA

by

David London
School of Geology and Geophysics
University of Oklahoma
Norman, OK 73019 USA

Michael E. Zolensky
Planetary Materials Branch
SN2/NASA
Johnston Space Center
Houston, TX 77058 USA

Edwin Roedder
U. S. Geological Survey
National Center, Mail Stop 959
Reston, VA 22092 USA

Canadian Mineralogist, in press

ABSTRACT

Diomignite, $Li_2B_4O_7$, occurs as a clear, colorless, pseudo-rhombohedral daughter mineral ($\leq$ 30 μm in maximum dimension) in crystal-rich fluid inclusions in spodumene from the Tanco pegmatite, Bernic Lake, Manitoba. The identity of diomignite was established by a variety of analytical techniques, with final confirmation based on the identical X-ray Gandolfi camera diffraction data for diomignite and synthetic $Li_2B_4O_7$. Optics are: uniaxial (-) for diomignite and synthetic $Li_2B_4O_7$; ω = 1.612(2), ε = 1.554(2), δ = 0.058(4) for synthetic $Li_2B_4O_7$. Cell parameters for diomignite are $\underline{a}$ = 9.470(4) Å, $\underline{c}$ = 10.279(5) Å, refined in the tetragonal space group $\underline{I4_1cd}$; $\underline{V}$(cell) = 921.83(1) Å^3, Z = 8, $\underline{V}$(mole) = 69.397 cc, d(calc) = 2.437 g/cc. Five strongest x-ray lines are 4.07 Å (I = 100; index = 112), 2.662 Å (60; 123), 3.495 Å (50; 022), 2.587 Å (40; 132), and 2.045 Å (40; 332). Natural diomignite and $Li_2B_4O_7$ synthesized at high $\underline{P}$ and $\underline{T}$ display pseudo-rhombohedral forms $\{10\bar{1}1\}$ and $\{10\bar{1}0\}$ of the pseudo-symmetric crystal class 32/m. The apparent rhombohedral forms can be reconciled with the tetragonal space group by shortening of a {100} tetragonal prism, and angular intersections of $[\underline{0k0}] \wedge [\underline{hkl}]$ of approximately 60°.

Recognition of a $Li_2B_4O_7$ (diomignite) component in an aluminosilicate-rich daughter mineral assemblage has important consequences for the physicochemical properties and crystallization sequence for late-stage fluids in Li- and B-rich rare-element pegmatites such as Tanco. The diomignite component serves as a flux to depress solidus temperatures, to increase

silicate fluid - H_2O miscibility, and to enhance the solubilities of ore-forming incompatible lithophile elements in late-stage pegmatitic fluids.

KEYWORDS: lithium, boron, alkali tetraborate, granite, pegmatite, melt properties, volatile components, rare elements

INTRODUCTION

A study of fluid inclusions in spodumene from the Tanco pegmatite, Bernic Lake, Manitoba, has revealed the presence of a complex assemblage of daughter minerals (London 1982, 1983, 1984b, 1986a; London et al. 1982). This crystalline assemblage includes a highly birefringent, colorless, pseudo-rhombohedral phase that has subsequently been identified as the new mineral species diomignite, natural $Li_2B_4O_7$. The name diomignite stems from Homeric Greek dios mignen (divine mix), in allusion to the pronounced fluxing effects of $Li_2B_4O_7$ on the hydrous pegmatite magma. Type samples have been deposited in the Smithsonian Institution, National Museum of Natural History, Washington, D.C., and the American Museum of Natural History, New York, N.Y., in the form of doubly polished chips of spodumene that contain diomignite-bearing inclusions. The mineral name and species have received approval by the IMA Commission on New Minerals and Mineral Names. Diomignite is the first new mineral species to be described solely as a daughter mineral in fluid inclusions.

OCCURRENCE

Diomignite has been observed only as small ($\leq$ 30 μm) anhedral to euhedral crystals in fluid inclusions in spodumene, and tentatively in fluid inclusions in the petalite from which

most of the spodumene formed. In these associations, diomignite is an abundant and widely distributed phase; it occurs in virtually every crystal-rich inclusion in spodumene (Fig. 1A). Diomignite is a component of an assemblage of daughter minerals that includes albite, cookeite, quartz, pollucite-analcime solid solution, microlite, and an unidentified carbonate (Fig. 1B). Diomignite and associated daughter minerals are entirely absent from the abundant fluid inclusions in the quartz that formed contemporaneously with the spodumene (as spodumene + quartz pseudomorphs after petalite: Černý & Ferguson 1972). Evidence cited in London (1985) shows that the inclusions in quartz are secondary and are not contemporaneous with those in spodumene.

IDENTIFICATION

The fine grain-size of diomignite, its location in fluid inclusions as loosely attached crystals, and its composition make the characterization difficult and incomplete in that no definitive chemical analysis could have been performed. The data presented below, however, are sufficiently diagnostic that little doubt remains as to the identity or composition of the phase.

In doubly polished plates of spodumene, diomignite can be readily recognized by its high mean index of refraction and high birefringence (Fig. 1, Table 1). Euhedral crystals generally show pseudo-rhombohedral forms which can be interpreted as combinations of a rhombohedron $\{10\bar{1}1\}$ and short hexagonal prism $\{10\bar{1}0\}$. Cleavage and twinning have not been observed in diomignite.

Diomignite crystals on spodumene cleavage surfaces were examined by scanning and point mode electron microscopy (SEM) and energy dispersive spectroscopic (EDS) analysis at an accelerating voltage of 20 KeV, condenser current of 2.0 amps, and 100 seconds of live count time on an Si(Li) detector crystal (Fig. 1C). The EDS analyses of carbon-coated diomignite crystals show no detectable major or minor elements in any of several orientations with respect to the electron beam and detector-crystal geometries, thus providing confirmation that diomignite consists wholly of elements with atomic number less than 11. Additional delimiting information on the composition of diomignite was obtained from microthermometric solubility measurements in unopened fluid inclusions (London 1986a). The observed depression in the freezing point of the aqueous fluid that surrounds diomignite crystals is indicative of a low-salinity solution (cf. a solubility for $Li_2B_4O_7$ = 2.98 g/ 100 cm^3 cold water: Weast 1974; see London 1986a). Although complex and incomplete, the measured thermometric properties for synthetic $Li_2B_4O_7$-H_2O solutions also show a relatively small depression in the freezing point of -1.6(0.1)°C that is consistent with the microthermometric data on ~~rom~~ the aqueous phase in inclusions in the spodumene. Heating the inclusions to 350°C showed little rounding ~~the~~ corners or edges of diomignite crystals over the duration of the experiments (up to 30 minutes). The combined results of freezing and heating data show that diomignite, like $Li_2B_4O_7$, is sparingly soluble in an aqueous fluid medium. The diomignite daughter crystals are stable to T > 375°C, which

precludes sassolite, H_3BO_3, as a possible candidate. Sassolite decomposes incongruently at $\underline{T}$ > 170°C (Weast 1974). The aqueous fluids in the inclusions are saturated with respect to diomignite to approximately 420°C. In the system $Li_2B_4O_7$-H_2O, however, lithium tetraborate remains stable to higher P-T conditions. At P_{fluid} = 200 MPa, $Li_2B_4O_7$ melts congruently at 700°C (London 1983, 1986a).

In hydrothermal experiments in which diomignite dissolved and reacted with aluminosilicate phases to form glass on quench, no CO_2-rich fluid was evolved; thus, diomignite was shown not to be a carbonate. Fluid inclusions near the tips of large, primary spodumene laths do contain a carbonate in addition to diomignite (Fig. 1B). Where the two phases coexist, the carbonate usually can be distinguished from diomignite by the higher birefringence of the carbonate. In addition, the carbonate dissolves completely between 275°-300°C and yields a small amount of CO_2 fluid upon subsequent quench of the hydrothermal experiments.

A search for a highly birefringent non-carbonate phase that is slightly soluble in water, is stable to $\underline{T}$ > 375°C, and is composed wholly of elements lighter than sodium yielded very few possibilities among known inorganic compounds. Among these compounds, only $Li_2B_4O_7$ satisfies all of the available data on the optical and physical-chemical properties of diomignite. Confirmation of the identity of diomignite was obtained by Gandolfi X-ray diffraction patterns of single crystals. Diomignite crystals were extracted from fluid inclusions by the method described by Zolensky & Bodnar (1982). Single crystals

were x-rayed in a Gandolfi camera of diameter 57.3 mm using CuK(α) radiation generated at 40 kV, 20 mA, with a Ni foil filter, and a graphite monochromator. A single diomignite crystal mounted on a glass whisker was run for three days under vacuum. (Because of the length of exposure and the faintness of lines, the pattern for diomignite does not copy well. The original film pattern may be borrowed from the first author.) A crystalline Si standard was used to determine the camera constant. Corrections for film shrinkage proved to be unnecessary. The observed X-ray diffraction pattern (Table 2) is virtually identical to the powder patterns reported for synthetic $Li_2B_4O_7$ by Sastry & Hummel (1958), Krogh-Moe (1962), and in ~~Figure 2 and~~ Table 2. Individual reflection intensities of diomignite differ from those of synthetic $Li_2B_4O_7$ because the present study relied on single crystals of diomignite mounted in a Gandolfi camera. The X-ray data for synthetic $Li_2B_4O_7$ were obtained from powder patterns.

The space group of synthetic $Li_2B_4O_7$ is $I4_1cd$, and its cell parameters are a = 9.477 Å and c = 10.286 Å (Krogh-Moe 1962; Natarajan *et al.* 1979). A least-squares refinement of the Gandolfi camera data for diomignite using the program of Appleman and Evans (1973) yielded refined cell parameters that are in close agreement with those of Krogh-Moe (1962) for synthetic $Li_2B_4O_7$ (Table 1). The tetragonal space group and symmetry proposed by Krogh-Moe (1962) for synthetic $Li_2B_4O_7$, however, are inconsistent with the apparent hexagonal-rhombohedral forms of class 3 2/m displayed by diomignite and by $Li_2B_4O_7$ synthesized

from anhydrous melts at one atmosphere (Sastry & Hummel 1958). Some SEM images of $Li_2B_4O_7$ crystals synthesized at hydrothermal conditions possess ~~pseudo~~-rhombohedral forms (Fig. 2A), ~~but~~ these can be reconciled with a tetragonal symmetry by shortening of the {100} prism, and by angular intersections of {100} prism and {111} pyramid faces at approximately 60°. The tetragonal-appearing crystals in Figure 2B, however, possess mirror symmetry perpendicular to [001], and hence might belong to the tetragonal 4/m 2/m 2/m class. Synthetic $Li_2B_4O_7$ crystallized from aqueous solution at room P and T also appear to possess a symmetry consistent with 4/m 2/m 2/m (Fig. 2B).

We attempted in vain to obtain ion microprobe data for diomignite (with Dr. Erik Steele, analyst, National Bureau of Standards, Gaithersburg, MD). The crystals originally X-rayed by M.E.Z., however, had ~~popped~~ dropped off their whisker mounts and were lost. Efforts to locate diomignite crystals by ion microscopy in grain mounts were hampered by two factors: (1) the crushed host spodumene diluted the abundance of diomignite crystals by a factor of approximately 10^5, and (2) with the limited Z-direction focus on the Cameca IMS-3F ion probe, the topography of the grain mount surface was found to be too great for secondary ion imaging. We subsequently attempted to use an Ar ion mill to expose a diomignite-bearing inclusion near a polished surface of spodumene. Even the botryoidal surface produced by ion milling produced some dispersion of the secondary ion beam, and the dispersion and sample charging around inclusion walls precluded any degree of secondary beam focus. Further Ar ion milling to

minimize the relief of inclusion walls demonstrated that diomignite is more volatile in a charged Ar beam than is spodumene, and diomignite crystals were quickly cratered to oblivion.

SIGNIFICANCE OF NATURAL $Li_2B_4O_7$ IN PEGMATITE SYSTEMS

Diomignite and the associated aluminosilicate daughter minerals represent the crystallization products of a late-stage hydrous borosilicate fluid that was entrapped principally by spodumene that formed as a result of the breakdown of petalite -> spodumene + quartz. This reaction relationship was recognized at Tanco by Černý & Ferguson (1972) and has been confirmed experimentally by Stewart (1963, 1978), Munoz (1971), and London (1984a). The results of fluid inclusion microthermometry and other experimental data place entrapment conditions at 470°-500°C and 270-290 MPa, the P-T interval over which spodumene crystallized at Tanco (London 1986a). The $Li_2B_4O_7$ component of the natural fluid at Tanco apparently was responsible for substantial depression of solidus temperatures and for the increased reciprocal miscibility of silicate liquid and H_2O (London 1983, 1984b, 1986a). Hydrothermal phase equilbrium experiments in the analoguous synthetic system $LiAlSiO_4$-$NaAlSi_3O_8$-SiO_2-$Li_2B_4O_7$-H_2O show that $Li_2B_4O_7$ concentrations comparable to those of the inclusions in Tanco spodumene (see Table 2 in London 1986a) promote rapid rates of crystallization and significant reductions in fluid viscosity through

depolymerization of residual silicate fluids (London 1986a). The combined effects of Li and B on solidus depression and silicate-H_2O miscibility appear to be far greater than of either component by itself (cf. Chorlton & Martin 1978; Stewart 1978; Pichavant 1981; 1983; Martin 1983; Martin & Henderson 1984).

NMR spectroscopic studies of crystalline and amorphous borate compounds have shown a close correlation between the coordination of boron in crystals and in compositionally similar glasses (quenched melts)(e.g., Bray 1978). There are two BO_3^{3-} and two BO_4^{5-} clusters per formula unit of crystalline $Li_2B_4O_7$ (Krogh-Moe 1962; Natarajan et al. 1979). The presence of two BO_4^{5-} clusters per formula unit of $Li_2B_4O_7$ may be taken as an additional indication of the peralkaline composition of the late-stage fluids at Tanco (fluid inclusion contents have an agpaitic index of approximately 1.3: London, 1986a). The proportion of $[BO_4^{5-}]/[BO_3^{3-}]$ should increase with increasing fluid alkalinity (Pichavant 1984; London 1986a), as reflected by the following acid-base hydrolysis reactions:

$$^{III}BO_3^{3-} + OH^- = {}^{IV}BO_3(OH)_4^{\uparrow -} \qquad (1)$$

$$H^+ + {}^{IV}B(OH)_4^- = {}^{III}B(OH)_3 + H_2O \qquad (2)$$

and by the fact that tetrahedral BO_4^{5-} oxyanions are stronger Lewis bases than are triangular BO_3^{3-} clusters. Borosilicate minerals are monitors of alkalinity. Tourmaline, which may be stable with micas and topaz in comparatively acidic conditions, contains only triangular BO_3^{3-} clusters. Reedmergnerite,

$NaBSi_3O_8$, has been reported only from peralkaline igneous rocks (Pichavant et al. 1984) and contains only tetrahedral BO_4^{5-} oxyanions (Appleman and Clark 1965). Recently, Foord et al. (1986) have reported feldspars from tourmaline-rich pockets in granitic pegmatites from San Diego County, California, that contain approximately 50 mol % reedmergnerite. This association of B-rich feldspars with late-stage tourmaline-rich zones is a further indication of the presence of boron-rich peralkaline fluids in the final stages of consolidation of complex rare-element pegmatites.

The volumetric proportion of diomignite to other crystalline and fluid phases in the Tanco spodumene inclusions (approximately 10 vol. %) provides an indication of the boron contents that are obtainable through fractional crystallization of natural pegmatite magmas. The boron content of the Tanco inclusions is far in excess of that needed to produce Fe-rich tourmaline (schorl) in granitic systems (Pichavant 1981). The presence of diomignite in the Tanco inclusions bears evidence of high Li and B contents of late-stage fluids. It has been suggested that when tourmaline crystallized at Tanco, the diomignite component was extracted from the hydrous silicate fluid (London and Morgan, 1985; Morgan and London, 1985; London, 1986a). As a result, albite, micas, and other aluminosilicate and oxide-forming ores were deposited, leaving a comparatively low-density residual aqueous phase (London 1986a). The crystallization products of the hydrous borosilicate fluid at Tanco are represented by the

saccharoidal albite unit that contains economic concentrations of Ta-Sn-oxides and beryl in the eastern ore-zone (Černý 1982).

These observations from Tanco should be applicable to Li- and B-rich rare-element pegmatites elsewhere. The concentration of tourmaline in late-stage internal and wall rock assemblages in many massive and miarolitic pegmatites manifests the instability of tourmaline throughout much of the history of primary crystallization. In Li- and B-rich miarolitic pegmatites, unusually high concentrations of tourmaline and boron-rich feldspars (e.g., 2-3 wt. % B in K-feldspar: Foord et al. 1986) are found in gem-bearing pockets, which are the latest primary units to form (e.g., Foord 1977; London 1986b). Late-stage albite-mica-tourmaline zones contain most deposits of rare metals and gem minerals in pegmatites throughout the world. The enrichment of incompatible elements in such units may stem partly from high concentrations of the borate component in the parent fluid. Borate oxyanions may form stable complexes with high field-strength cations, and may remove them from network-forming sites in the aluminosilicate melt (e.g., Hess, 1980; Kawamoto et al., 1981; Ryerson, 1985; London 1986a). Loss of this fluxing component through crystallization of tourmaline or boron loss to wall rocks would promote the deposition of incompatible elements along with typical aluminosilicate components of rock-forming minerals (London 1986a).

Diomignite may be found in assemblages of daughter minerals (probably hosted by spodumene, topaz, and possibly beryl, all of

which tend to trap crystal-rich inclusions) in other Li- and B-rich pegmatites where the crystallization of tourmaline was a late-stage phenomenon. Diomignite, however, has not been (and probably will not be) identified as a constituent of tourmaline-rich pockets. The crystallization of Li-tourmaline consumes the diomignite component of late-stage fluids (London, 1986b). The precipitation of comparatively insoluble borates such as hambergite (e.g., in tourmaline-rich pockets of the Himalaya dike system, California: Foord 1977) would further reduce the activity of boron in late-stage fluids. Any excess $Li_2B_4O_7$ probably would be lost to wall rocks during pocket rupture or subsequently dissolved from pockets by the influx of externally derived fluids (e.g., see Foord et al. 1986).

To a large extent, the diomignite component ($Li_2B_4O_7$) in Li- and B-rich rare-element pegmatites may control the physicochemical properties of highly fractionated, late-stage fluids, and may be responsible for the accumulation and ultimate precipitation of rare-metal ores and gem minerals. The recognition of diomignite as a component of late-stage fluids has important implications for the genesis of Li- and B-rich rare-element pegmatites.

ACKNOWLEDGEMENTS

Thanks to Dr. Erik Steele, National Bureau of Standards, Gaithersburg, MD, for his efforts to obtain an ion microprobe

X-ray procedures were performed at the Department of ~~Earth Sciences~~ Geosciences, The Pennsylvania State University.

mass spectrum of diomignite. This research was supported in part by a U. S. Bureau of Mines Allotment Grant G-1154140 (Oklahoma Mining and Mineral Resources Research Institute, Robert H. Arndt, director), by the University of Oklahoma Research Council, and by a research fellowship to D. L. from the Atlantic Richfield Foundation. We thank P. Černý, R. F. Martin, and an anonymous reviewer for their constructive comments and careful editorial scrutiny.

REFERENCES

Appleman, D. E. & Clark, J. R. (1965): Crystal structure of reedmergnerite, a boron albite, and its relation to feldspar chemistry. Amer. Mineral. 50, 1827-1850.

Appleman, D. E. & Evans, H. T. Jr. (1973): Job 9214: indexing and least-squares refinement of powder diffraction data. U.S. Geol. Survey Computer Contrib. 20 (NTIS Doc PB2-16188).

Bray, P. J. (1978) NMR studies of borates. In L. D. Pye, V. D. Frenchette, & N. J. Kreidl, eds., Borate Glasses: Structure, Properties, Applications. Plenum Publishing Corporation, 321-351.

Černý, P. (1982): The Tanco pegmatite at Bernic Lake, southeastern Manitoba. In P. Černý, ed., Granitic Pegmatites in Science and Industry. Mineral Assoc. Canada Short Course Hndbk., 8 527-543.

Černý, P. & Ferguson, R. B. (1972): The Tanco pegmatite at Bernic Lake, Manitoba: IV. Petalite and spodumene relations. Can. Mineral. 11, 660-678.

Chorlton, L. B. & Martin, R. F. (1978): The effect of boron on the granite solidus. Can. Mineral. 16, 239-244.

Foord, E. E. (1977): Famous mineral localities. The Himalaya dike system, Mesa Grande district, San Diego County, California. Mineral. Rec. 8, 461-474.

Foord, E. E., Starkey, H. C., & Taggart, J. E. (1986): Mineralogy and paragenesis of "pocket" clays and associated

minerals in complex granitic pegmatites, San Diego County, California. Amer. Mineral. in press.

Hess, P. C. (1980): Polymerization model for silicate melts. In R. B. Hargraves, ed., Physics of Magmatic Processes. Princeton University Press, 3-48.

Kawamoto, Y., Clemens, K., and Tomozawa, M. (1981): Effects of MoO_3 on phase separation of Na_2O-B_2O_3-SiO_2 glasses. Jour. Amer. Ceram. Soc., 64, 292-296.

Krogh-Moe, J. (1962): The crystal structure of lithium diborate, Li_2O-$2B_2O_3$. Acta Cryst. 15, 190-193.

London, D. (1982): Fluid-solid inclusions in spodumene from the Tanco pegmatite, Bernic Lake, Manitoba. (abs.) Geol. Soc. Amer. Abs. Prog. 14 (7), 549.

London, D. (1983): The magmatic - hydrothermal transition in rare-metal pegmatites: fluid inclusion evidence from the Tanco mine, Manitoba. (abs.) Trans. Amer. Geophys. Union 64, 874.

London, D. (1984a): Experimental phase equilibria in the system $LiAlSiO_4$-SiO_2-H_2O: a petrogenetic grid for lithium-rich pegmatites. Amer. Mineral. 69, 995-1004.

London, D. (1984b): The role of lithium and boron in fluid evolution and ore deposition in rare-metal pegmatites. (abs). Geol Soc. Amer. Abs. Prog. 16 (6), 578.

London, D. (1985): Origin and significance of inclusions in quartz: a cautionary example from the Tanco pegmatite, Manitoba. Econ. Geol. 80, 1988-1995.

London, D. (1986a): The magmatic - hydrothermal transition in the Tanco rare-element pegmatite: evidence from fluid inclusions and phase equilibrium experiments. Amer. Mineral., Jahns Memorial Issue, in press.

London, D. (1986b): Formation of tourmaline-rich gem pockets in miarolitic pegmatites. Amer. Mineral., Jahns Memorial Issue, in press.

London, D. and Morgan, G. B., VI (1985): Wall rock alteration around the Tanco rare-element pegmatite, Manitoba: relations to pegmatite evolution. (abs.) Trans. Amer. Geophys. Union, 66, 1154.

London, D., Spooner, E. T. C., & Roedder, E. (1982): Fluid - solid inclusions in spodumene from the Tanco pegmatite, Bernic Lake, Manitoba. Carnegie Inst. Washington Yr. Bk. 81, 334-339.

Martin, J. S. (1983): An experimental study of the effects of lithium on the granite system. J. Ussher Soc. 5, 417-420.

Martin, J. S. & Henderson, C. M. B. (1984): An experimental study of the effects of small amounts of lithium on the granite system. Nat. Environ. Res. Council, Publ. Ser. D, no. 25, 30-35.

Morgan, G. B., VI, and London, D. (1985): Wall rock alteration around the Tanco rare-element pegmatite, Manitoba: petrology of alteration halos: (abs.) Trans. Amer. Geophys. Union, 66, 1153-1154.

Munoz, J. L. (1971): Hydrothermal stability relations of synthetic lepidolite. Amer. Mineral. 56, 2069-2087.

Natarajan, M., Faggiani, R. & Brown, I. D. (1979): Lithium tetraborate, $Li_2B_4O_7$. Cryst. Struct. Comm. 8, 367.

Pichavant, M. (1981): An experimental study of the effect of boron on a water-saturated haplogranite at 1 kbar vapour pressure. Contrib. Mineral. Petrol. 76, 430-439.

Pichavant. M. (1983): Melt-fluid interaction deduced from from studies of silicate-B_2O_3-H_2O systems at 1 kbar. Bull. Mineral. 106, 201-211.

Pichavant. M., Schnapper, D., & Brown, W. L. (184): Al = B substitution in alkali feldpsars: Preliminary hydrothermal data in the system $NaAlSi_3O_8$ - $NaBSi_3O_8$. Bull. Mineral. 107, 529-537.

Ryerson, F. J. (1985): Oxide solution mechanisms in silicate melts: Systematic variations in the activity coefficient of SiO_2. Geochim. Cosmochim. Acta, 49, 637-649.

Sastry, B. S. R., & Hummel, F. A. (1958): Studies in lithium oxide systems: I. $Li_2O{\cdot}B_2O_3$-B_2O_3. Jour. Amer. Ceram. Soc. 41, 7-17.

Stewart, D. B. (1963): Petrogenesis and mineral assemblages of lithium-rich pegmatites. (abs.) Geol. Soc. Amer. Spec. Pap. 76, 159.

Stewart, D. B. (1978): Petrogenesis of lithium-rich pegmatites. Amer. Mineral. 63, 970-980.

Weast, R. C., Ed. (1974): Handbook of Physics and Chemistry, 54th ed. Chem. Rubber Co. Press.

Zolensky, M. E. & Bodnar, R. J. (1982): Identification of fluid inclusion daughter minerals using Gandolfi x-ray techniques. Amer. Mineral. 67, 137-141.

CAPTIONS TO FIGURES

Figure 1. (A) Doubly polished chip of spodumene (partly crossed polars) from Tanco, illustrating the size, distribution and contents of crystal-rich, diomignite-bearing inclusions. (B) Photomicrograph (partly crossed polars) of a diomignite-bearing inclusion in coarse-grained spodumene from Tanco. Photographs (A) and (B) reprinted from London (1986a). (C) SEM image of a diomignite-bearing inclusion. In addition to diomignite (d) the inclusion contains quartz (a), albite (b), and cookeite (c). Photograph (C) reprinted from London et al. (1982).

Figure 2. SEM images of synthetic $Li_2B_4O_7$ crystallized at 600°C and 200 MPa_{H2O} (A) and at room temperature and pressure (B). Apparent tetragonal forms are prism {100} and pyramid {111}. The forms are appropriate for the 4/m 2/m 2/m crystal class. The presence of {100} forms gives diomignite and high-temperature synthetic $Li_2B_4O_7$ a pseudo-rhombohedral appearance in some orientations. The {100} prism is rarely developed or absent in $Li_2B_4O_7$ crystals sythesized at room temperature and pressure. Scale bar in both photos is 10 micrometers.

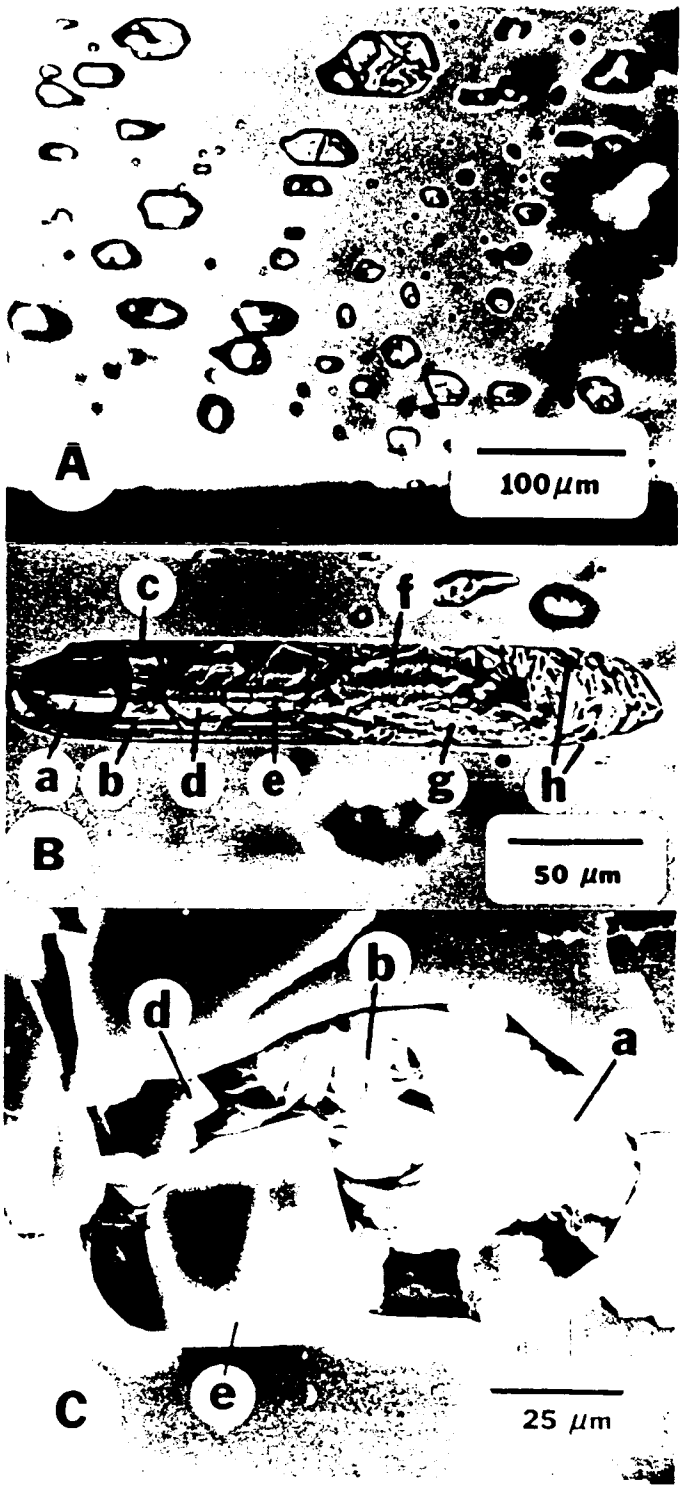
A
100μm
c
f
a
b
d
e
g
h
B
50 μm
b
d
a
C
e
25 μm

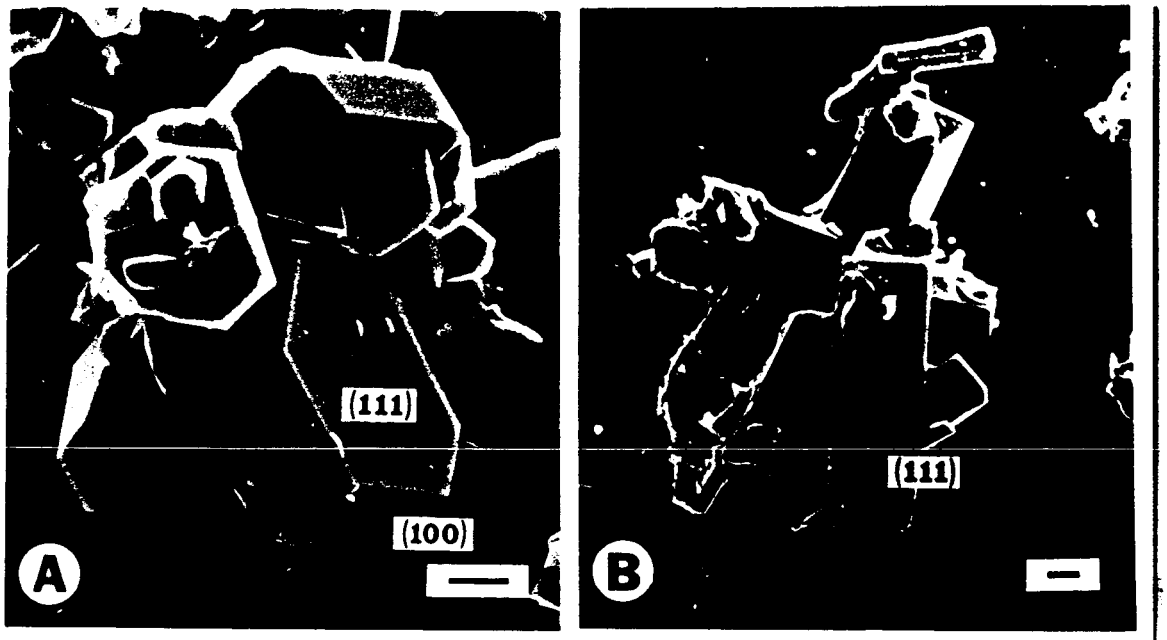
[111]
[100]
A
[111]
B

Table 1. Optical and physical properties of Tanco diomignite and synthetic $Li_2B_4O_7$

	diomignite	synthetic $Li_2B_4O_7$		
		Sastry and Hummel (1958)	Krogh-Moe (1962)	London*
Optics:				
Indicatrix	uniaxial (-)	uniaxial (-)		uniaxial (-)
R.I.	high ($\bar{n} \sim 1.6$)	$\omega = 1.605(2)$**		$\omega = 1.612(1)$
		$\epsilon = 1.560(2)$		$\epsilon = 1.554(2)$
Birefringence	high ($\delta \sim 0.05$)	$\delta = 0.045(4)$		$\delta = 0.058(4)$
Unit Cell:				
Space Group	$I4_1cd$	$I4_1cd$	$I4_1cd$***	$I4_1cd$
Cell Parameters	a = 9.470(4) Å	a = 9.470 Å	a = 9.477(3) Å	a = 9.464(3) Å
	c = 10.279(5) Å	c = 10.278 Å	c = 10.286(4) Å	c = 10.275(4) Å
V(cell)	921.83(1) Å^3	921.7 Å^3	923.82(1) Å^3	920.30(1) Å^3
Z	8	8	8	8
Physical Properties:				
Molar Volume	69.397 cc	69.387 cc	69.546 cc	69.281 cc
Density (calc)	2.437 g/cc	2.437	2.432 g/cc	2.441
Crystal Forms	pyramid {111}	hexagonal		pyramid {111}
	prism {100}			prism {100}

*This report; see Figure 2
**Standard deviation to last significant figure
***tetragonal space group assigned by Krogh-Moe (1962)

Table 2. X-ray powder diffraction data for Tanco diomignite and synthetic $Li_2B_4O_7$

hkl	d_{calc}(Å)*	diomignite d_{obs}(Å)	diomignite I/I_o	synthetic $Li_2B_4O_7$ d_{obs}(Å)+	synthetic $Li_2B_4O_7$ I/I_o+	synthetic $Li_2B_4O_7$ d_{obs}(Å)**	synthetic $Li_2B_4O_7$ I/I_o**
020	4.735	4.73	10	4.74	8	4.72	8
012	4.517	4.51	10	--	--	4.51	1
112	4.077	4.07	100	4.08	100	4.07	100
121	3.916	3.908	20	3.918	18	3.914	18
022	3.482	3.495	50	3.485	40	3.486	40
130	2.995	--	--	2.997	2	2.995	2
123	2.664	2.662	60	2.665	40	2.662	40
132	2.588	2.587	40	2.589	55	2.587	55
004	2.570	--	--	2.571	6	2.568	6
231	2.545	2.545	10	2.547	8	2.545	8
040	2.368	2.370	5	2.369	6	2.360	6
024	2.259	--	--	2.261	2	--	--
141	2.242	2.240	20	2.243	14	2.240	14
042	2.150	--	--	2.152	4	2.152	4
240	2.118	--	--	2.119	4	2.117	4
233	2.085	2.085	20	2.086	10	2.084	10
332	2.047	2.045	40	2.049	25	2.047	25
224	2.039	--	--	2.040	12	2.039	12
242	1.958	1.957	20	1.959	10	1.954	10
134	1.950	1.952	10	1.951	8	1.950	8
143	1.908	1.910	10	1.909	10	1.903	10
341	1.863	--	--	1.864	2	1.862	2
150	1.857	1.852	5	1.858	2	1.856	2
125	1.849	--	--	1.851	4	1.850	4
152	1.747	--	--	1.748	2	1.749	2
044	1.741	--	--	1.742	4	1.745	4
251	1.733	1.734	10	1.734	8	1.731	8
116	1.660	1.657	5	1.660	8	1.658	8
				plus 13 more lines		plus additional lines	

* indexed using the program Unit Cell (Appleman and Evans, 1973).

\+ Krogh-Moe, 1962.

** synthesis at 600°C, 2 kbar $P(H_2O)$; see Figure 2.